Natriuretic peptides block synaptic transmission by activating phosphodiesterase 2A and reducing presynaptic PKA activity

Fei Hu[a,b], Jing Ren[b,c], Ju-en Zhang[b,d], Weixin Zhong[b], and Minmin Luo[a,b,d,1]

[a]Graduate School of Peking Union Medical College, Beijing 100730, China; [b]National Institute of Biological Sciences, Beijing 102206, China; [c]College of Life Sciences, Beijing Normal University, Beijing 100875, China; and [d]School of Life Sciences, Tsinghua University, Beijing 100084, China

Edited* by Paul W. Sternberg, California Institute of Technology, Pasadena, CA, and approved September 14, 2012 (received for review June 4, 2012)

The heart peptide hormone atrial natriuretic peptide (ANP) regulates blood pressure by stimulating guanylyl cyclase-A to produce cyclic guanosine monophosphate (cGMP). ANP and guanylyl cyclase-A are also expressed in many brain areas, but their physiological functions and downstream signaling pathways remain enigmatic. Here we investigated the physiological functions of ANP signaling in the neural pathway from the medial habenula (MHb) to the interpeduncular nucleus (IPN). Biochemical assays indicate that ANP increases cGMP accumulation in the IPN of mouse brain slices. Using optogenetic stimulation and electrophysiological recordings, we show that both ANP and brain natriuretic peptide profoundly block glutamate release from MHb neurons. Pharmacological applications reveal that this blockade is mediated by phosphodiesterase 2A (PDE2A) but not by cGMP-stimulated protein kinase-G or cGMP-sensitive cyclic nucleotide-gated channels. In addition, focal infusion of ANP into the IPN enhances stress-induced analgesia, and the enhancement is prevented by PDE2A inhibitors. PDE2A is richly expressed in the axonal terminals of MHb neurons, and its activation by cGMP depletes cyclic adenosine monophosphates. The inhibitory effect of ANP on glutamate release is reversed by selectively activating protein kinase A. These results demonstrate strong presynaptic inhibition by natriuretic peptides in the brain and suggest important physiological and behavioral roles of PDE2A in modulating neurotransmitter release by negative crosstalk between cGMP-signaling and cyclic adenosine monophosphate-signaling pathways.

presynaptic modulator | neurotransmission | ChannelRhodopsin 2

Synaptic transmission is dynamically modulated by neuropeptides, which often act on receptors that belong to the G protein-coupled receptor (GPCR) family (1). In addition to GPCRs, a unique family of receptors known as membrane guanylyl cyclases (GCs) can be activated by neuropeptides such as natriuretic peptides to catalyze the intracellular production of cyclic guanosine monophosphate (cGMP) (2, 3). In animals across taxa, cGMP signals influence cellular physiology by acting on cGMP-stimulated protein kinase G (PKG), cyclic nucleotide-gated (CNG) channels, or cGMP-sensitive phosphodiesterases (PDEs) (3, 4). In *Caenorhabditis elegans*, a membrane GC acts on the presynaptic terminals of olfactory neurons to induce a behavioral switch (5). Several membrane GCs and their associated peptide ligands are expressed in the mammalian brain. For example, GC-C is activated by the gut peptide hormones guanylin and uroguanylin to amplify postsynaptic responses of midbrain dopamine neurons (6). Another member of the membrane GC family, GC-A (also named NPR-A), is the receptor for atrial natriuretic peptide (ANP) and brain natriuretic peptide (BNP), and its activation reduces blood pressure and volume in the cardiovascular system (7–9). Both natriuretic peptides and their receptors are expressed in several discrete brain areas (10–13), but it remains unclear how ANP affects behaviors and modulates synaptic transmission in the brain.

One of the most prominent brain areas expressing GC-A is the projection from the medial habenula (MHb) in the epithalamus to the interpeduncular nucleus (IPN) in the midbrain (Fig. 1*A*). This neural pathway links forebrain limbic areas with midbrain modulatory systems and regulates a diverse array of behaviors including pain, anxiety, sleep, and nicotine addiction (14–16). Abundant GC-A mRNA is detected in MHb neurons (17). In addition, strong ANP binding is observed in the IPN (12, 13), which receives dense innervation from the MHb (18, 19). Thus, GC-A is likely expressed in the axonal terminals of MHb neurons and may regulate neurotransmitter release from MHb neurons to IPN neurons.

In this study, we optogenetically activate the MHb-to-IPN pathway and examine whether ANP affects evoked transmitter release and, if so, by which signal transduction cascade (Fig. 1*B*). We took advantage of ChAT-ChR2-EYFP mice, which allowed us to selectively stimulate the axonal terminals of MHb neurons with light and evoke fast glutamatergic responses in IPN neurons (19). We first demonstrated that natriuretic peptides strongly suppress neurotransmitter release. We then tested whether the presynaptic inhibition is mediated by the activity of PKG, CNG channels, or PDEs. After finding that phosphodiesterase 2A (PDE2A) plays an essential role in the ANP effect on synaptic transmission, we went on to show that PDE2A activity negatively regulates the cyclic adenosine monophosphates (cAMP)-signaling pathway. The results from these experiments reveal strong effects of natriuretic peptides on neurotransmitter release and suggest important roles of presynaptic crosstalk between cGMP and cAMP signals in modulating synaptic transmission.

Results

ANP Application Blocks Glutamate Transmission. We confirmed the functional presence of ANP receptors in the IPN by assaying cGMP accumulation in mouse brain slices (Fig. S1). ELISA revealed that application of PDE inhibitors enhanced cGMP accumulation, and ANP application further increased cGMP levels approximately threefold (Fig. 1*C*), suggesting that ANP activates guanylyl cyclase and that PDEs are constitutively active in the IPN. We then asked how ANP could influence neurotransmitter release by performing whole-cell patch recordings from IPN neurons of ChAT-ChR2-EYFP transgenic mice (Fig. S1*D*). In these mice, ChannelRhodopsin 2 (ChR2) is expressed in the so-called "cholinergic" neurons in the MHb, which project their axons to the dorsal and central subnuclei of the IPN (19). Our previous recordings have shown that brief light stimulation of ChR2+ axonal terminals in the IPN produces fast glutamatergic excitatory

Author contributions: F.H. and M.L. designed research; F.H., J.R., J.-e.Z., and W.Z. performed research; F.H., W.Z., and M.L. analyzed data; and F.H. and M.L. wrote the paper.

The authors declare no conflict of interest.

*This Direct Submission article had a prearranged editor.

[1]To whom correspondence should be addressed. E-mail: luominmin@nibs.ac.cn.

This article contains supporting information online at www.pnas.org/lookup/suppl/doi:10.1073/pnas.1209185109/-/DCSupplemental.

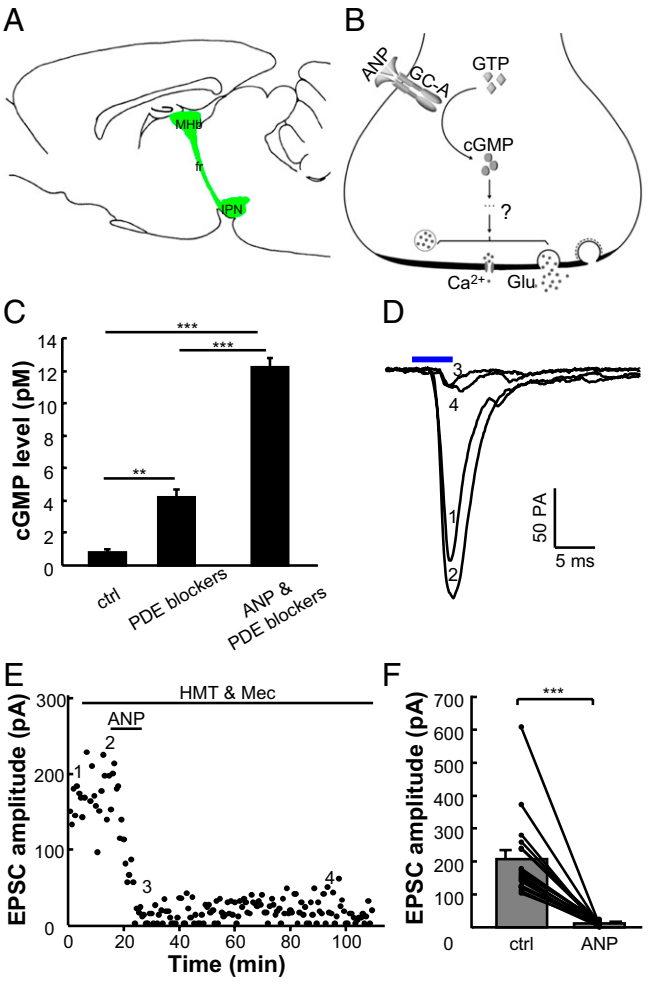

Fig. 1. ANP profoundly inhibits evoked release of glutamate from the axonal terminals of MHb neurons to the IPN. (*A*) A schematic drawing shows the axonal projection from the MHb to the IPN via the fiber tract fasciculus retroflexus (fr). (*B*) A cartoon illustrating the major aim of this study, which was to identify the potential effect of ANP on glutamate (Glu) release and the underlying signal transduction pathways. (*C*) PDE inhibitors (10 μM BAY 60–7550 and 1 mM IBMX) increased cGMP accumulation in the IPN, and ANP application further stimulated cGMP production in the IPN (**$P < 0.01$; ***$P < 0.001$; within-group *t* tests; $n = 4$ separate readings for each group). (*D* and *E*) Representative physiological traces (*D*) and the plot of EPSC amplitude versus time (*E*) show that ANP application (100 nM) completely abolishes fast EPSCs evoked by brief light illumination (5 ms; blue bar). An EPSC in an IPN neuron was evoked by light stimulation (1), and the application of the nAChR blockers hexamethonium (HMT, 50 μM) and mecamylamine (Mec, 5 μM) slightly increased its amplitude (2). Addition of ANP into bath solution blocked the EPSC (3), and this blockade lasted for over 1 h in wash solution (4). Each trace in *D* represents the average of eight sweeps from the times indicated in *E*. (*F*) Summary data show that ANP essentially eliminates fast EPSCs (***$P < 0.001$; paired *t* test; $n = 18$ cells). Separate lines represent data from individual neurons; "ctrl" indicates EPSCs measured in nAChR blockers. (*C* and *F*) Error bars indicate SEM.

postsynaptic potentials (EPSCs), whereas tetanic stimulation generates slow cholinergic responses (19).

We chose to analyze the effects of ANP application only on fast glutamatergic EPSCs with peak amplitudes over 100 pA for their stability. Because of the difficulty in obtaining stable cholinergic EPSCs with repetitive episodes of tetanic stimulation, the effect of ANP on acetylcholine release was not examined in this study. Axonal terminals were stimulated by 5-ms blue light pulses using an optical fiber with its tip directly above the IPN. As cGMPs can also be generated by soluble GCs (sGCs) following the stimulation of nitric oxide (NO), we applied the nitric oxide synthase blocker Nω-Nitro-L-arginine methyl ester hydrochloride (L-NAME) to exclude the potential effects of NO/sGC signaling. The $GABA_A$-receptor blocker picrotoxin was also added to the bath solution to eliminate GABAergic currents. Consistent with the glutamatergic nature of the fast EPSCs (19), brief light stimulation evoked EPSCs that were resistant to the application of a mixture of two nAChR antagonists (hexamethonium and mecamylamine) (Fig. 1*D*). Strikingly, bath perfusion of ANP (100 nM) resulted in an immediate reduction in the fast EPCSs, leading to an almost complete abolishment of EPSCs in all cells tested after 10 min of ANP treatment (reduction ratio = 95%; Fig. 1 *D–F*). ANP at a lower concentration (10 nM) produced ~65% reduction and was partially reversible with washing (Fig. S2 *A* and *B*), suggesting a dose-dependent inhibition of EPSCs. Light-evoked EPSCs were similarly blocked by BNP (500 nM; Fig. S2 *C* and *D*), which activates GC-A with a lower affinity (20).

We examined whether ANP acted pre- or postsynaptically. To test whether the ANP effect resulted from postsynaptic actions on IPN neurons, we measured excitatory currents evoked by puffing the glutamate receptor agonist AMPA before and after ANP application in the presence of the sodium channel blocker tetrodotoxin (TTX). ANP did not change the AMPA currents (Fig. S2 *E* and *F*). Cell-attached recordings from IPN neurons revealed that ANP did not affect action potential firing frequency in response to AMPA application (Fig. S2 *G* and *H*). In addition, ANP application did not affect the amplitude or frequency of spontaneous EPSCs recorded in IPN neurons, which likely receive glutamatergic inputs from sources in addition to the MHb (Fig. S2 *I–L*). In rat pituitary and vasopressin neurons, natriuretic peptides can affect neuronal intrinsic properties by opening potassium channels (21, 22). We directly recorded from MHb neurons to examine whether ANP could target the somata of MHb neurons and affect their intrinsic excitability. Pressure injection of ANP did not elicit any currents, and bath perfusion did not affect the intrinsic properties or synaptic responses of MHb neurons (Fig. S2 *M–O*). These results indicate that neither inactivation of postsynaptic receptors in the IPN nor inhibition of neuronal firing at the somata of MHb neurons is responsible for the blockade of glutamate neurotransmission, suggesting that the ANP effect results from GC-A activity in presynaptic axonal terminals.

Synaptic Blockade Effect of ANP Is Mediated by PDE2A. cGMP molecules can activate the cGMP-sensitive kinase PKG or CNG channels to regulate a broad set of physiological processes (3, 4). We applied membrane-permeable PKG inhibitors to test whether PKG activity is required for ANP to reduce glutamatergic synaptic transmission. ANP maintained its ability to block glutamate transmission following preincubation in KT5823 (2 μM), an inhibitor that interferes with the PKG catalytic domain (Fig. 2 *A* and *B*). In the presence of KT5823, ANP application reduced EPSC amplitude by ~90% ($n = 6$ cells; Fig. 2*C*), which is comparable to the reduction amplitude without KT5823 (Fig. 1*F*). Similarly, ANP reduced EPSCs by over 90% following preincubation in Rp-8-pCPT-cGMP (10 μM), a PKG inhibitor acting on the enzyme regulatory domain ($n = 7$ cells; Fig. S3 *A* and *B*). In addition, the amplitude of evoked EPSCs was not reduced by bath perfusion of two membrane-permeable PKG activators (100 μM 8-pCPT-cGMP or 200 μM 8-Br-cGMP; Fig. S3 *C–F*). The failure of PKG inhibitors to prevent the neurotransmission blockade by ANP and the inability of two PKG activators to mimic ANP suggest a minimal role of PKG in mediating the presynaptic inhibition of glutamate release following GC-A activation. Furthermore, blocking the cGMP-sensitive CNG channel with L-*cis*-diltiazem (10 μM) did not affect the presynaptic inhibition of EPSCs by ANP (Fig. 2 *D–F*), suggesting that CNG channels also do not mediate the ANP effect.

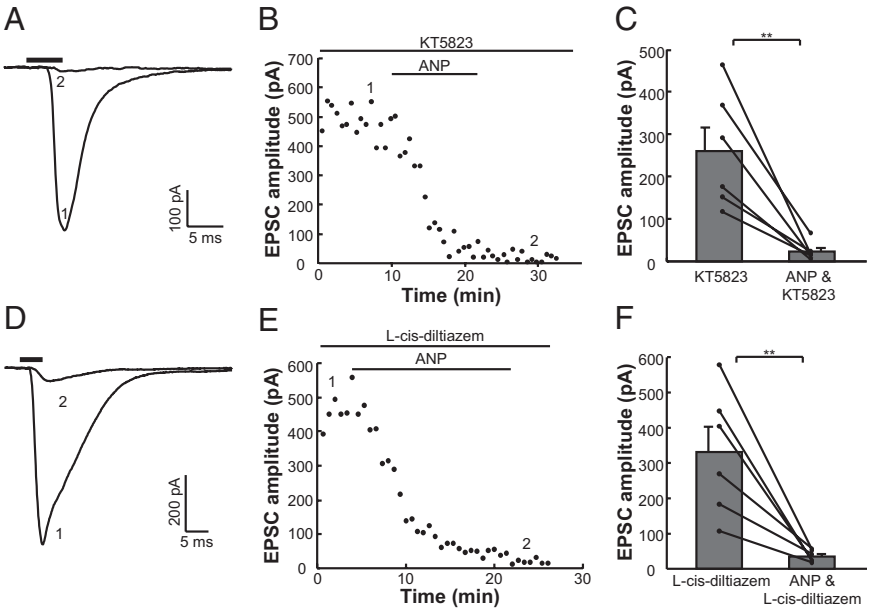

Fig. 2. Blockade of glutamate transmission by ANP does not depend on the activity of PKG or CNG channels. (*A* and *B*) ANP remains effective in blocking glutamate transmission following the pretreatment of the PKG-specific inhibitor KT5823 (2 μM). A fast glutamatergic EPSC was recorded in the presence of the nAChR blockers HMT and Mec and the PKG inhibitor KT5823 (1), and the addition of ANP remained potent in abolishing the EPSC (2). The same conventions were as in Fig. 1 *D* and *E*. (*C*) Summary data show that ANP remains capable of abolishing the fast EPSCs in the presence of KT5823 (**$P <$ 0.01; paired *t* test; $n = 6$ cells). (*D*–*F*) Representative trace (*D*) and time course of EPSC amplitude (*E*) in a single cell as well as population data (*F*) showing that the application of L-*cis*-diltiazem (10 μM) does not block the inhibitory effect of ANP on EPSCs (**$P <$ 0.01; paired *t* test; $n = 6$ cells). (*C* and *F*) Error bars indicate SEM.

In addition to PKG and CNG channels, some PDEs are stimulated by cGMP signals. For example, PDE2A is stimulated by cGMP to hydrolyze both cGMPs and cAMPs (23). Efforts in studying PDE2A functions have been facilitated by the development of several selective PDE2A inhibitors, including 2-(3,4-dimethoxybenzyl)-7-{(1R)-1-[(1R)-1-hydroxyethyl]-4-phenylbutyl}-5-methyllimidazo[5,1-f][1,2,4]triazin-4(3H)-one (labeled as BAY 60–7550 for simplicity) and erythro-9-(2-hydroxy-3-nonyl)adenine (EHNA) (24). The fast EPSCs evoked by light stimulation were potentiated by nearly threefold from basal levels after bath application of BAY 60–7550 (1 μM) (Fig. 3 *A*–*C*). Moreover, preincubation in BAY 60–7550 largely eliminated the effect of ANP on reducing fast EPSCs. The potentiated currents were eliminated by the AMPA-type glutamate receptor antagonist CNQX (10 μM), demonstrating that they are glutamatergic in nature (Fig. 3*B*). Even in the presence of ANP, BAY 60–7550 enabled rapid reversal of EPSCs following the blockade by CNQX (Fig. 3*B*), further suggesting an antagonism of the ANP effect by BAY 60–7550. Similarly, light-evoked EPSCs were potentiated and their blockade by ANP was largely prevented by EHNA (Fig. S4 *A* and *B*), another commonly used PDE2A inhibitor (24). The efficacy of both PDE2A inhibitors on blocking ANP effects strongly suggests that PDE2A serves as the downstream transducer of cGMP signals produced by GC-A activation.

We asked whether ANP influences behaviors and whether PDE2A inhibitors can block the behavioral effects of ANP. Because the MHb is implicated in regulating behaviors related to pain and stress (25), we infused ANP into the IPN to examine its effects on nociceptive responses in behaving mice (Fig. S4*C*). In hot-plate tests, ANP infusion alone did not change the latency of behavioral response to heat (Fig. 3*D*). Challenging mice with forced swimming, which could induce stress-induced analgesia (SIA), indeed increased the response latency. In this stress-related pain behavioral paradigm, the hot-plate latency was further lengthened following ANP injection into the IPN. In addition, this lengthening of the response latency was blocked by infusion of BAY 60–7750 into the IPN before testing (Fig. 3*D*). These results thus suggest that ANP potentiates SIA by modulating the

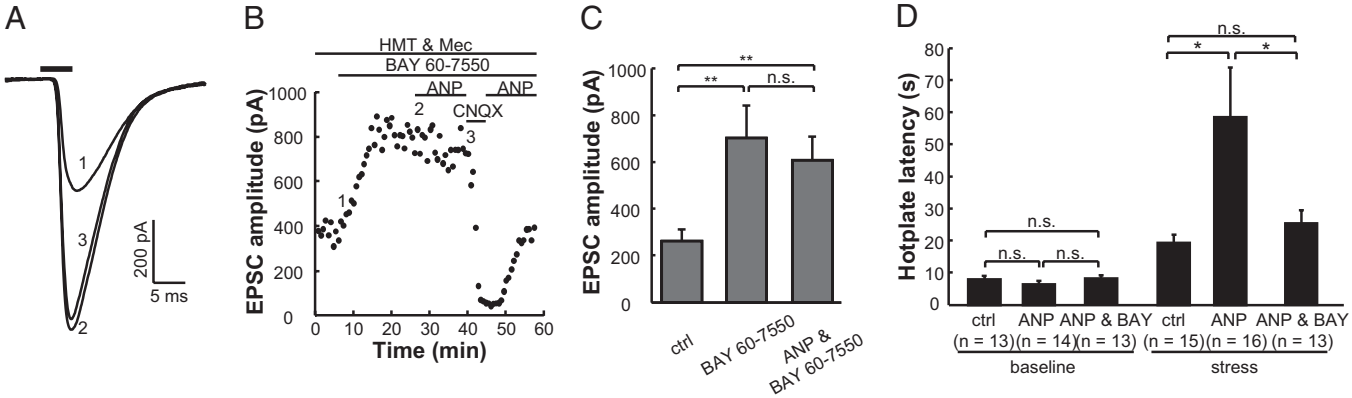

Fig. 3. PDE2A mediates the physiological and behavioral functions of ANP in the MHb-IPN pathway. (*A*–*C*) A representative single cell (*A* and *B*) and summary data (*C*) illustrate that BAY 60–7550, a selective PDE2A inhibitor, potentiates fast EPSCs and largely prevents ANP from blocking them (**$P < 0.01$; n.s., not significant, $P = 0.063$; $n = 10$ cells). (*D*) Hot-plate response latency for mice injected with aCSF ("ctrl"), ANP, or a mixture of ANP and BAY 60–7550 before and after the stress of forced swimming and hot-plate tests. ANP or the mixture of ANP and BAY 60–7550 did not change hot-plate latency at basal states. Forced swimming increased hot-plate latency, suggesting SIA. ANP potentiated the stress-induced analgesia effect, and this enhancement was blocked by the addition of BAY 60–7550 (*$P \leq 0.05$; between-group *t* test; numbers of test mice are shown below the drug name for each group). (*C* and *D*) Error bars indicate SEM.

physiological properties of the MHb–IPN pathway. In addition, the behavioral effect of ANP requires the activity of PDE2A.

An earlier study reports PDE2A expression in the MHb and IPN (26), but it was unclear whether PDE2A is specifically expressed in the axonal terminals of MHb neurons. We observed PDE2A immunoreactivity in the somata of MHb neurons (Fig. S5 *A* and *B*). In the IPN, PDE2A was expressed only in the synaptic terminals (Fig. 4 *A* and *B* and Fig. S5*C*). PDE2A expression was restricted to ChR2-EYFP+ axonal terminals in the dorsal and central IPN subnuclei (Fig. 4*B* and Fig. S5*C*), which are targeted by the axonal projection from MHb cholinergic neurons (18, 19).

Because both cGMPs and cAMPs are the substrates of PDE2A (23), we asked whether ANP application could reduce presynaptic cAMP levels via PDE2A activity. ELISA measurements revealed that ANP significantly reduced the cAMP concentrations in the IPN to less than half of basal levels, and this reduction was prevented by blocking PDE2A activity with BAY 60–7550 pretreatment (Fig. 4*C*). BAY 60–7750 alone increased cAMP levels by over fourfold, supporting the role of PDE2A in suppressing constitutive cAMP accumulation and thus transmitter release (Fig. 3). Moreover, ANP substantially reduced cAMP levels following the stimulation of adenylyl cyclase by forskolin, and this reduction was blocked by BAY 60–7550 pretreatment (Fig. 4*D*).

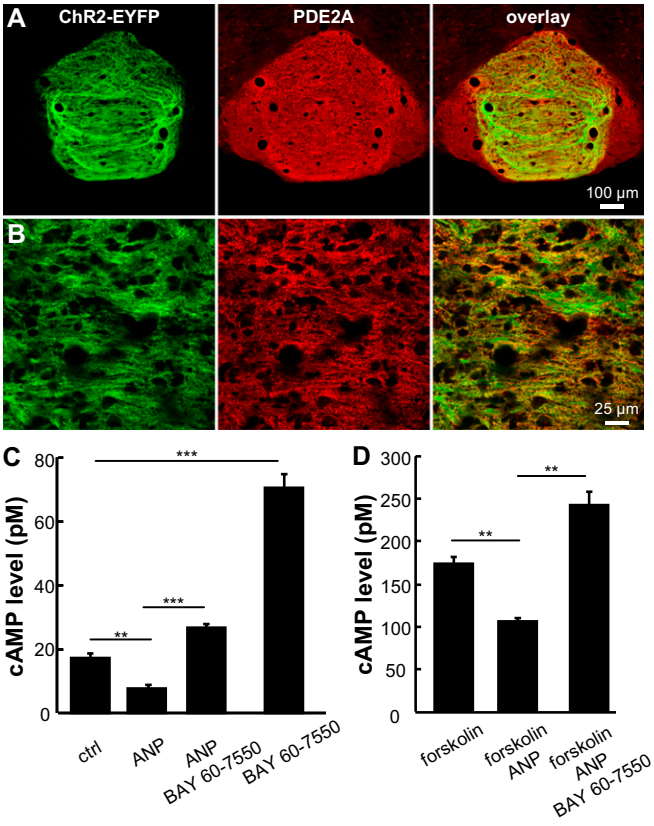

Fig. 4. PDE2A is richly expressed in the axonal terminals of MHb neurons and negatively regulates cAMP levels in the IPN. (*A*) Confocal image of a coronal section from a ChAT-ChR2-EYFP mouse showing the expression of PDE2A (red) in ChR2-EYFP+ terminals (green) in the IPN. (*B*) High-magnification views show that essentially all ChR2-EYFP-labeled axonal terminals (green) are immunopositive for PDE2A (red) in the IPN. (*C* and *D*) ANP substantially reduces basal (*C*) and forskolin (25 μM)-evoked (*D*) cAMP levels in the IPN, and this reduction is reversed by blocking PDE2A with BAY 60–7750 (10 μM). Application of the PDE2A blocker alone increases cAMP levels (**$P < 0.01$; ***$P < 0.001$; within-group *t* tests; $n = 4$ separate readings for each group). (*C* and *D*) Error bars indicate SEM.

These biochemical measurements thus demonstrate that ANP can activate PDE2A to efficiently reduce cAMP levels in the IPN.

Effect of ANP Is Likely Produced by Depleting Protein Kinase A Activity. We investigated how PDE2A shapes downstream signals to block glutamate transmission. Both the cAMP-sensitive protein kinase A (PKA) and the exchange protein activated by cAMP (Epac) have been implicated in modulating neurotransmitter release in various brain areas (27). By applying the membrane-permeable PKA activator 6-BNZ-cAMP, we tested whether direct PKA activation could rescue fast EPSCs following their blockade by ANP. For all cells tested ($n = 6$ cells), EPSCs were blocked by ANP and then fully recovered after bath application of 6-BNZ-cAMP (Fig. 5 *A*–*C*). In current-clamp mode, 6-BNZ-cAMP reversed the ANP blockade and enabled IPN neurons to be depolarized and fire action potentials in response to light stimulation (Fig. S6*A*). In contrast to the effectiveness of the PKA activator 6-BNZ-cAMP, application of the selective Epac activator 8-CPT-2Me-cAMP failed to reverse the ANP blockade (Fig. S6 *B* and *C*).

We used PKA inhibitors to further examine the role of basal PKA activity in regulating glutamate release. EPSCs were reduced by ∼70% after bath perfusion of a mixture of PKA inhibitors (H89 and Rp-8-Br-cAMP; Fig. 5 *D* and *E*). The residual current may be explained by an insufficient ability of PKA inhibitors to fully block intracellular PKA activity after permeating the cell membrane. Additional analyses show that PKA inhibitors did not affect the frequency or amplitude of spontaneous EPSCs in IPN neurons (Fig. S6 *D*–*G*), indicating that the substantial suppression of EPSCs by PKA inhibitors results from changes in presynaptic terminals but not in postsynaptic neurons.

Discussion

Since their original discovery in 1980s (7–9, 13), natriuretic peptides and their receptors have been found to be richly expressed in several brain areas (12, 13, 17). However, their physiological functions as well as the underlying signaling mechanisms in the brain remain poorly understood. In this study, we find that ANP application in the IPN abolishes synaptic release of glutamate from habenular axonal terminals. Furthermore, we show that the ANP effects are mediated by PDE2A activity, which in turn depletes cAMP and thus eliminates basal PKA activity. Our data demonstrate a strong effect of presynaptic inhibition by natriuretic peptides and delineate a signaling pathway through which cGMP signals block neurotransmitter release by negatively coupling to cAMP pathways (Fig. 5*F*).

ANP or BNP produces an almost complete blockade of glutamate release by MHb neurons, indicating that they are very strong presynaptic inhibitors. The inhibitory effects of natriuretic peptides appear much weaker in other areas of the nervous system. In the C-fibers from the dorsal root ganglia, BNP reduces glutamatergic EPSCs by ∼30% (28). ANP weakens EPSCs by 46% for the connection between osmoreceptor neurons in the organum vasculosum laminae terminalis and the magnocellular neurosecretory cells in the supraoptic nucleus (29). In the retina, BNP functions as a postsynaptic modulator and produces a roughly 40% suppression of $GABA_A$-receptor–mediated inhibitory currents in bipolar cells (30).

Our results differ from previous studies that highlight a pivotal role of PKG in mediating the effect of natriuretic peptides in the dorsal root ganglia and the retina (28, 30). For the connection between the MHb and IPN, PKG blockers do not disrupt the shut-off effect of ANP, and PKG activators do not change EPSCs. In contrast, ANP is completely antagonized by PDE2A blockers. Biochemical and imaging studies of culture cells have shown that PDE2A is capable of efficiently depleting cAMPs following cGMP stimulation (23, 31). Our biochemical assays show that ANP reduces cAMP levels in the IPN area of brain slices and that this reduction is fully blocked by applying PDE2A inhibitors. In addition, presynaptic inhibition of glutamate release by ANP is reversed by a PKA activator, and the ANP effect is largely

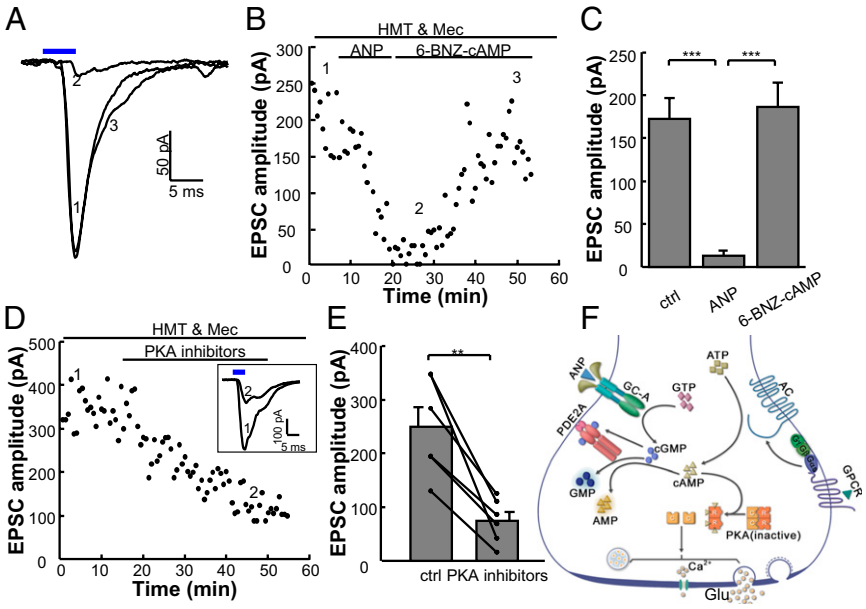

Fig. 5. The ANP/GC-A/PDE2A–signaling pathway is mediated by PKA activity. (*A*–*C*) Data from a representative cell (*A* and *B*) and group data (*C*) show that the ANP-induced inhibition is reversed by 6-BNZ-cAMP (50 μM), a specific PKA activator (***$P < 0.001$; paired *t* test; $n = 6$ cells). (*D* and *E*) PKA inhibitors substantially reduces the amplitudes of fast EPSCs (**$P < 0.01$; $n = 6$ cells). *Inset* in *D* shows representative traces before and after the application of PKA inhibitors. (*C* and *E*) Error bars indicate SEM. (*F*) Diagram illustrating the potential signal transduction pathway mediating presynaptic inhibition by ANP. At the basal level, cAMP is constitutively produced by GPCR/adenylyl cyclase (AC) pathways and activates PKA to phosphorylate certain components essential for glutamate (Glu) release. Upon ANP binding, GC-A produces cGMP and in turn activates PDE2A to hydrolyze both cGMP and cAMP. Hydrolysis of cAMP depletes PKA activity and blocks glutamate release. PDE2A metabolizes cGMP to compartmentalize and terminate the cGMP signals.

mimicked by PKA inhibitors. These results indicate that ANP blocks neurotransmission by depleting presynaptic cAMP concentrations. Interestingly, the signal transduction cascade in the axonal terminals of MHb neurons is reminiscent of that in nonneuronal cells in the periphery. In both adrenal glomerulosa cells and cardiac myocytes, ANP activates its receptors to produce cGMPs, which in turn stimulate PDE2A to reduce intracellular cAMP levels (32–34). Therefore, negative crosstalk between cGMP and cAMP cascades might be one of the conserved mechanisms underlying natriuretic peptide action both inside and outside the nervous system. PDE2A has been thought to serve simply as a cGMP scavenger in olfactory CO_2 neurons (35, 36). Our physiological recordings suggest that PDE2A performs the important function of regulating neurotransmitter release by negatively linking cGMP signals to the cAMP pathway.

The MHb–IPN pathway is believed to be related to anxiety and nicotine addiction (14, 15). Our behavioral tests indicate that ANP enhances stress-induced analgesia in a PDE2A-dependent manner. This finding is consistent with the facts that the MHb receives input from forebrain septal areas that are involved in stress-related behaviors and that MHb neurons express opiate receptors (18, 25). The exact sources of ANP or BNP in the IPN remain unclear. An early study indicated that ANP may be expressed by MHb neurons (11), suggesting the possibility of presynaptic inhibition by autocrine signaling of ANP. Alternatively, ANP might be transported to the IPN following their production in the heart. Although the exact behavioral context for ANP release into the IPN remains unclear, our results suggest that the ANP signaling can regulate animal behaviors by modulating neurotransmission in the habenulo-interpeduncular pathway. Furthermore, the powerful and selective PDE2A inhibitors have contributed to the elucidation of PDE2A functions but have not yet been put into clinical use (24, 37, 38). We propose that PDE2A inhibitors could be used as pharmacological drugs for treatment of anxiety and nicotine addiction via their actions on MHb axonal terminals.

The efficacy of a PKA activator in reversing ANP-induced presynaptic inhibition supports an essential role of PKA in transmitter release. cAMP can modulate Ca^{2+}-dependent exocytosis of secretory cells by acting through PKA- or Epac-dependent signaling pathways (27). In cerebellar and hippocampal synapses, cAMP signals facilitate transmitter release by acting on PKA (39, 40). At the calyx synapse of Held, the potentiatory effect of cAMP requires the activity of Epac but not PKA (41). In the axonal terminals of MHb neurons, the ANP effect is reversed by a PKA activator but not by a Epac activator, suggesting that certain proteins critical for exocytosis are phosphorylated by endogenous PKA activity in the basal state and that such phosphorylation is required for neurotransmitter release. In addition, the fact that PDE2A inhibitors potentiate glutamatergic EPSCs indicates that increasing cAMP levels may further enhance PKA activity and facilitate vesicle release. In the cortex and many other brain areas, neurotransmitter release is often presynaptically modulated by the activity of GPCRs that influence intracellular cAMP levels (1). The striking inhibitory effect of natriuretic peptides illustrates the power of cGMP signals in shutting off neurotransmitter release by depleting presynaptic cAMP levels through cGMP-stimulated dual substrate PDEs such as PDE2A.

Materials and Methods

Mice. Experimental protocols were approved by the Animal Care and Use Committee of the National Institute of Biological Sciences, Beijing, and conformed to governmental policies. We used adult ChAT-ChR2-EYFP mice (6–12 wk, 18–25 g) of either sex for physiological recordings and C57BL/6 mice (8–12 wk, males) for behavioral tests. The ChAT-ChR2-EYFP mice were a gift of G. Feng (Massachusetts Institute of Technology, Cambridge, MA) and have been characterized in detail (19).

Slice Preparation, Electrophysiology, Photostimulation, and Drug Application. The methods of slice preparation and whole-cell patch recordings were identical to what was described in our previous study (19). For cell-attached recordings, the pipettes were filled with 150 mM NaCl. Physiological traces were low-pass-filtered at 2.6 kHz, digitized at 10 kHz, and analyzed using a commercial recording system (MultiClamp 700B and Clampfit 10, Molecular Devices). For recording fast EPSCs, neurons were held at −60 or −65 mV. We averaged the amplitudes of five to eight sweeps for each data point. EPSCs amplitudes were measured by subtracting the mean of a 1- to 2-ms window around the peak with the mean of a 10-ms window immediately before light stimulation. Summary data are presented as mean ± SEM. A level of $P < 0.05$ was used to designate a difference as statistically significant.

For light stimulation, blue light pulses (473 nm) were generated by a diode-pumped solid-state 473-nm laser and delivered by an optical fiber (200-μm core diameter, N.A. = 0.22). The tip of the optical fiber was submerged in artificial cerebrospinal fluid (aCSF) and placed ∼1.5 mm above the recording site, resulting in a light intensity of 0.2–20 mW/mm^2. Generation of light pulses (5 ms) was digitally controlled with Digidata 1440 (Molecular Devices).

The following drugs were added to the superfusion medium by dilution of stock solutions: ANP (10 or 100 nM; Sigma), BAY 60–7550 (1 μM; Cayman Chemical), BNP (500 nM; Sigma), 6-BNZ-cAMP (50 μM; Sigma), 8-Br-cGMP

(200 μM; Sigma), 8-CPT-2Me-cAMP (50 μM; Tocris), 8-pCPT-cGMP (100 μM; Sigma), CNQX or DNQX (10 μM; Sigma), L-*cis*-Diltiazem (10 μM; Biomol), EHNA (90 μM; Sigma), H89 (30 μM; Sigma) and Rp-8-Br-cAMP (170 μM; Biolog), KT5823 (2 μM; Biomol), L-NAME (100 μM; Sigma), picrotoxin (50 μM; Sigma), Rp-8-pCPT-cGMP (10 μM; Biomol), TTX (1 μM; Sigma), and a mixture of hexamethonium-Cl (50 μM; Sigma) and mecamylamine (5 μM; Sigma). The effectiveness of Rp-8-pCPT-cGMP, KT5823, 8-Br-cGMP, and L-*cis*-Diltiazem has been confirmed by recent studies in our group (6, 35). AMPA (17.5 μM; Sigma) and acetylcholine (1 mM; Sigma) were pressure-ejected using an eight-channel drug delivery system (MPS-1, Inbio Life Science Instrument), with the tip of the drug delivery pipette located ~500 μm away from the recording site. Picrotoxin and L-NAME was added to the recording solution to block $GABA_A$-receptor–mediated transmission and the effects mediated by sGCs. At least 5 min of baseline was collected from each cell.

Measurement of cGMP and cAMP Levels. Brain slices (250 μm thick) containing the IPN were prepared from ChAT-ChR2-EYPF mice and recovered in oxygenated aCSF for 40 min at 34 °C. The tissues were then incubated with the following drugs for 20 min: ANP (100 nM), BAY60-7550 (10 μM), forskolin (25 μM), and 3-isobutyl-1-methylxanthine (IBMX; 1 mM). The IPN area was dissected out under the visual guidance of fluorescent microscopy and lysed with 0.1 mM HCl for 5 min. Tissues were further disrupted with an ultrasound probe for 10 min and centrifuged (14,000 × *g*) at 4 °C for 10 min. The concentrations of cGMP or cAMP in the supernatant were measured with ELISA kits (NewEast Biosciences Inc., catalog no. 80101 or 80202).

Histology and Confocal Imaging. Cells were filled with Neurobiotin (0.25%; Vector Laboratories) in the intrapipette recording solution. Brain slices after recordings were fixed with 4% (wt/vol) paraformaldehyde in 0.1 M PBS, and neurons were stained with Cy3-conjugated streptavidin (1:500; 2 h) in 0.1 M PBS with 0.3% Triton-X. For PDE2A immunostaining, adult mouse brain was fixed and cryoprotected in 30% (wt/vol) sucrose. Frozen tissue was sectioned coronally at 40 μm thickness with a microtome (Leica CM 1900). After rinsing with 0.3% Triton-X in 0.1 M PBS and blocking with 2% (wt/vol) normal bovine serum for 1 h, sections were incubated with a rabbit anti-PDE2A antibody in the blocking solutions (1:200, 12 h in 4 °C; FabGennix Inc., PD2A-101AP). After rinsing, sections were then incubated with Cy3-conjugated goat anti-rabbit antibody for 2 h at room temperature (1:500; Jackson ImmunoResearch). Fluorescent images were acquired by a Carl Zeiss 510 confocal microscope.

Behavioral Assays. Mice were anesthetized with pentobarbital (80 mg/kg i.p.), and a guide cannula was implanted with its tip 0.5 mm above the IPN. One week later, mice were first exposed to forced swimming in a glass cylinder partially filled with 22–25 °C water for 8 min. After a 2-d recovery, drug or aCSF control (1 μL) was infused into the IPN through an internal cannula for 10 min (RWD202 Syringe Pump, RWD Life Science). Seven minutes later, mice were placed on a hot plate (Taimeng Technology), the temperature of which was set at 54.5 ± 0.5 °C. We assessed the baseline nociception response by measuring the latency to first hindpaw licking, tapping, or four-paw jumping. To test the effect of SIA the next day, all mice were injected with aCSF or drugs into the IPN and immediately immersed in cold water (4 °C) for 2 min. To measure the effect of BAY 60–7550 on ANP (10 μM)-induced SIA enhancement, we first injected 0.5 μL of BAY 60–7550 (25 μM) and then a 0.5-μL mixture of ANP (20 μM) and BAY 60–7550 (25 μM). Mice were then dried with paper towels and rested for 3 min before the hot-plate test.

ACKNOWLEDGMENTS. We thank G. Feng (Massachusetts Institute of Technology) for ChAT-ChR2-EYFP mice and Z. Liu and C. Qin (National Institute of Biological Sciences) for help with behavioral assays. M.L. is supported by China Ministry of Science and Technology 973 Grant 2010CB833902.

1. Miller RJ (1998) Presynaptic receptors. *Annu Rev Pharmacol Toxicol* 38:201–227.
2. Lucas KA, et al. (2000) Guanylyl cyclases and signaling by cyclic GMP. *Pharmacol Rev* 52(3):375–414.
3. Potter LR, Yoder AR, Flora DR, Antos LK, Dickey DM (2009) Natriuretic peptides: Their structures, receptors, physiologic functions and therapeutic applications. *Handb Exp Pharmacol* 191:341–366.
4. Reaume CJ, Sokolowski MB (2009) cGMP-dependent protein kinase as a modifier of behaviour. *Handb Exp Pharmacol* 191:423–443.
5. Tsunozaki M, Chalasani SH, Bargmann CI (2008) A behavioral switch: cGMP and PKC signaling in olfactory neurons reverses odor preference in C. elegans. *Neuron* 59(6):959–971.
6. Gong R, et al. (2011) Role for the membrane receptor guanylyl cyclase-C in attention deficiency and hyperactive behavior. *Science* 333(6049):1642–1646.
7. de Bold AJ (1985) Atrial natriuretic factor: A hormone produced by the heart. *Science* 230(4727):767–770.
8. Lang RE, et al. (1985) Atrial natriuretic factor: A circulating hormone stimulated by volume loading. *Nature* 314(6008):264–266.
9. Chinkers M, et al. (1989) A membrane form of guanylate cyclase is an atrial natriuretic peptide receptor. *Nature* 338(6210):78–83.
10. Saper CB, et al. (1985) Atriopeptin-immunoreactive neurons in the brain: Presence in cardiovascular regulatory areas. *Science* 227(4690):1047–1049.
11. Skofitsch G, Jacobowitz DM, Eskay RL, Zamir N (1985) Distribution of atrial natriuretic factor-like immunoreactive neurons in the rat brain. *Neuroscience* 16(4):917–948.
12. Quirion R, Dalpé M, Dam TV (1986) Characterization and distribution of receptors for the atrial natriuretic peptides in mammalian brain. *Proc Natl Acad Sci USA* 83(1):174–178.
13. Gibson TR, Wildey GM, Manaker S, Glembotski CC (1986) Autoradiographic localization and characterization of atrial natriuretic peptide binding sites in the rat central nervous system and adrenal gland. *J Neurosci* 6(7):2004–2011.
14. Fowler CD, Lu Q, Johnson PM, Marks MJ, Kenny PJ (2011) Habenular α5 nicotinic receptor subunit signalling controls nicotine intake. *Nature* 471(7340):597–601.
15. Agetsuma M, et al. (2010) The habenula is crucial for experience-dependent modification of fear responses in zebrafish. *Nat Neurosci* 13(11):1354–1356.
16. Hikosaka O (2010) The habenula: From stress evasion to value-based decision-making. *Nat Rev Neurosci* 11(7):503–513.
17. Herman JP, Dolgas CM, Rucker D, Langub MC, Jr. (1996) Localization of natriuretic peptide-activated guanylate cyclase mRNAs in the rat brain. *J Comp Neurol* 369(2):165–187.
18. Qin C, Luo M (2009) Neurochemical phenotypes of the afferent and efferent projections of the mouse medial habenula. *Neuroscience* 161(3):827–837.
19. Ren J, et al. (2011) Habenula "cholinergic" neurons co-release glutamate and acetylcholine and activate postsynaptic neurons via distinct transmission modes. *Neuron* 69(3):445–452.
20. Suga S, et al. (1992) Receptor selectivity of natriuretic peptide family, atrial natriuretic peptide, brain natriuretic peptide, and C-type natriuretic peptide. *Endocrinology* 130 (1):229–239.
21. Standaert DG, Cechetto DF, Needleman P, Saper CB (1987) Inhibition of the firing of vasopressin neurons by atriopeptin. *Nature* 329(6135):151–153.
22. White RE, et al. (1993) Potassium channel stimulation by natriuretic peptides through cGMP-dependent dephosphorylation. *Nature* 361(6409):263–266.
23. Martins TJ, Mumby MC, Beavo JA (1982) Purification and characterization of a cyclic GMP-stimulated cyclic nucleotide phosphodiesterase from bovine tissues. *J Biol Chem* 257(4):1973–1979.
24. Boess FG, et al. (2004) Inhibition of phosphodiesterase 2 increases neuronal cGMP, synaptic plasticity and memory performance. *Neuropharmacology* 47(7):1081–1092.
25. Herkenham M, Pert CB (1980) In vitro autoradiography of opiate receptors in rat brain suggests loci of "opiatergic" pathways. *Proc Natl Acad Sci USA* 77(9):5532–5536.
26. Juilfs DM, Soderling S, Burns F, Beavo JA (1999) Cyclic GMP as substrate and regulator of cyclic nucleotide phosphodiesterases (PDEs). *Rev Physiol Biochem Pharmacol* 135:67–104.
27. Seino S, Shibasaki T (2005) PKA-dependent and PKA-independent pathways for cAMP-regulated exocytosis. *Physiol Rev* 85(4):1303–1342.
28. Zhang FX, et al. (2010) Inhibition of inflammatory pain by activating B-type natriuretic peptide signal pathway in nociceptive sensory neurons. *J Neurosci* 30(32): 10927–10938.
29. Richard D, Bourque CW (1996) Atrial natriuretic peptide modulates synaptic transmission from osmoreceptor afferents to the supraoptic nucleus. *J Neurosci* 16 (23):7526–7532.
30. Yu YC, Cao LH, Yang XL (2006) Modulation by brain natriuretic peptide of GABA receptors on rat retinal ON-type bipolar cells. *J Neurosci* 26(2):696–707.
31. Nikolaev VO, Gambaryan S, Engelhardt S, Walter U, Lohse MJ (2005) Real-time monitoring of the PDE2 activity of live cells: Hormone-stimulated cAMP hydrolysis is faster than hormone-stimulated cAMP synthesis. *J Biol Chem* 280(3):1716–1719.
32. MacFarland RT, Zelus BD, Beavo JA (1991) High concentrations of a cGMP-stimulated phosphodiesterase mediate ANP-induced decreases in cAMP and steroidogenesis in adrenal glomerulosa cells. *J Biol Chem* 266(1):136–142.
33. Méry PF, Pavoine C, Pecker F, Fischmeister R (1995) Erythro-9-(2-hydroxy-3-nonyl)adenine inhibits cyclic GMP-stimulated phosphodiesterase in isolated cardiac myocytes. *Mol Pharmacol* 48(1):121–130.
34. Vandecasteele G, Verde I, Rücker-Martin C, Donzeau-Gouge P, Fischmeister R (2001) Cyclic GMP regulation of the L-type Ca(2+) channel current in human atrial myocytes. *J Physiol* 533(Pt 2):329–340.
35. Hu J, et al. (2007) Detection of near-atmospheric concentrations of CO2 by an olfactory subsystem in the mouse. *Science* 317(5840):953–957.
36. Luo M, Sun L, Hu J (2009) Neural detection of gases—carbon dioxide, oxygen—in vertebrates and invertebrates. *Curr Opin Neurobiol* 19(4):354–361.
37. Masood A, Nadeem A, Mustafa SJ, O'Donnell JM (2008) Reversal of oxidative stress-induced anxiety by inhibition of phosphodiesterase-2 in mice. *J Pharmacol Exp Ther* 326(2):369–379.
38. Menniti FS, Faraci WS, Schmidt CJ (2006) Phosphodiesterases in the CNS: Targets for drug development. *Nat Rev Drug Discov* 5(8):660–670.
39. Greengard P, Jen J, Nairn AC, Stevens CF (1991) Enhancement of the glutamate response by cAMP-dependent protein kinase in hippocampal neurons. *Science* 253 (5024):1135–1138.
40. Salin PA, Malenka RC, Nicoll RA (1996) Cyclic AMP mediates a presynaptic form of LTP at cerebellar parallel fiber synapses. *Neuron* 16(4):797–803.
41. Sakaba T, Neher E (2003) Direct modulation of synaptic vesicle priming by GABA(B) receptor activation at a glutamatergic synapse. *Nature* 424(6950):775–778.